Experimental Investigation of the Root Cause Mechanism and Effectiveness of Mitigating Actions for Axial Offset Anomaly in Pressurized Water Reactors

DOE Contract Number: DE-FG07-02ID14324

Final Technical Report

for the period June 1, 2002 – May 31, 2005

Principal Investigator: Said I. Abdel-Khalik
Nuclear Engineering Program
G.W. Woodruff School of Mechanical Engineering
Georgia Institute of Technology

July 2nd, 2005

SUMMARY

Axial offset anomaly (AOA) in pressurized water reactors refers to the presence of a significantly larger measured negative axial offset deviation than predicted by core design calculations. The neutron flux depression in the upper half of high-power rods experiencing significant subcooled boiling is believed to be caused by the concentration of boron species within the crud layer formed on the cladding surface. Recent investigations of the root-cause mechanism for AOA [1, 2] suggest that boron build-up on the fuel is caused by precipitation of lithium metaborate ($LiBO_2$) within the crud in regions of subcooled boiling. Indirect evidence in support of this hypothesis was inferred from operating experience at Callaway, where lithium return and hide-out were, respectively, observed following power reductions and power increases when AOA was present. However, **direct** evidence of lithium metaborate precipitation within the crud has, heretofore, not been shown because of its retrograde solubility. To this end, this investigation has been undertaken in order to **directly** verify or refute the proposed root-cause mechanism of AOA, and examine the effectiveness of possible mitigating actions to limit its impact in high power PWR cores.

A total of forty eight experiments ranging in duration from one day to nearly two months have been conducted in a pressure vessel at prototypical PWR primary coolant pressures and temperatures corresponding to core regions experiencing AOA. The concentrations of boron, lithium, hydrogen, and oxygen in the coolant were controlled and maintained at prototypical PWR values corresponding to beginning-of-cycle conditions. Electrically-heated Zircaloy-4 test elements were immersed in the coolant for the duration of the experiments (up to sixty one days), while maintaining them at specified constant surface heat fluxes up to 5×10^5 Btu/hr-ft^2 (~1.6 MW/m^2); these heat fluxes are comparable to those present at the hot spot in a modern, high-duty, four-loop PWR core. Nearly one third of the experiments were conducted while the coolant was forced to flow past the heated surface (forced convection/subcooled flow boiling), while the remaining experiments were conducted under natural convection/subcooled pool boiling conditions. In nearly two-thirds of the experiments, soluble and insoluble corrosion products (iron and nickel compounds) were added to the coolant in order to accelerate in-situ crud deposition, thereby making it possible to collect prototypical data within a reasonable time period (experiments are a few weeks long as opposed to the several months required for plants to develop AOA).

At the end of each experiment, the test elements were rapidly isolated from the coolant by discharging the entire system coolant inventory (i.e. rapidly blowing-down the system inventory to an external tank at atmospheric pressure) and simultaneously terminating power, thereby preventing the dissolution of any boron-bearing species which may be present within the crud, without causing surface burnout. Following each experiment, the test element was removed from the pressure vessel; analyses were then performed to determine the mass, thickness, composition, and overall morphology of the crud deposited on the surface, as well as the chemical composition and amount of boron-bearing species deposited within the crud. Experiments were conducted at different values of surface heat flux, exposure time, pH, coolant subcooling, soluble and insoluble iron and nickel concentrations, and initial surface conditions. Early experiments utilized test elements pre-coated with a nickel ferrite layer simulating the deposited crud. For later experiments, the addition of both soluble and insoluble iron and nickel

compounds promoted in-situ formation of crud; crud with prototypical composition, thickness, and morphology was consistently formed in those experiments. Upon conclusion of each experiment, analyses were performed to identify the boron hideout species, verify the presence or absence of lithium metaborate, and quantify the amount of boron-bearing material deposited within the crud.

The data obtained in this research indicate that the experimental technique used in this investigation can be successfully used to form PWR crud with prototypical composition and morphology, and that the boron-bearing species deposited in the crud can be successfully captured using the rapid blow-down technique. Significant amounts of boron were deposited in many experiments with in-situ formed crud; analyses of these deposits indicate that lithium tetra-borate, $Li_2B_4O_7$ (Diomignite), may be the dominant boron deposition species. This result is consistent with earlier work performed at Georgia Tech which suggests that the lithium-to-boron ratio in the deposited boron species is less than unity (i.e. less than the value for lithium metaborate). The data also suggest that operation at moderately elevated pH_T (~ 7.7) can significantly retard crud deposition, and hence, boron accumulation. This result is consistent with recent suggestions by industry to increase the pH levels for operating PWRs.

The quantitative data obtained in this investigation can be used to verify the validity of proposed mechanistic models for crud and boron deposition; these models can then be incorporated within mass-balance-based AOA assessment codes such as the BOA code widely used by industry [3]. In addition to the experimental data obtained during this investigation, this research has been used to train and educate students in areas of direct engineering interest to the nuclear power industry, including reactor operations, thermal-hydraulics, reactor chemistry, and core physics. The research offered students the opportunity to utilize state-of-the-art analytical techniques such as EDX, XRD, SIMS, and ICPMS. Four graduate students participated in this investigation. Three students have already graduated (one PhD in Nuclear Engineering, one MS in Nuclear Engineering, and one MS in Mechanical Engineering who is a minority student), while the fourth student continues to pursue his PhD degree in Nuclear Engineering.

CONTENTS

1. OBJECTIVES AND SCOPE OF EFFORT

The purpose of this investigation is to experimentally identify the nature of the boron hideout species associated with AOA in pressurized water reactors; such direct evidence will either support or refute the proposed root-cause mechanism based on $LiBO_2$ deposition within the crud. In addition, the experiments can provide the necessary experimental database to validate models for the net rate of boron deposition within the crud as a function of crud layer characteristics, exposure time, and operating conditions. Additionally, the effectiveness of various mitigating features to limit the extent of AOA in high power PWR cores will be explored.

Another major objective of this project is to educate graduate students in nuclear engineering who are interested in performing experimentally-based graduate theses in areas of direct relevance to designers and operators of water-cooled reactors as they push the state of the art towards longer operating cycles and higher power cores. Students interested in a wide range of areas, including reactor engineering, boiling heat transfer, mass transfer, corrosion, water chemistry, and reactor operations can directly benefit from such research. Graduate students perform theses research in the following two areas:

(a) Obtain quantitative data for the rate of crud and boron deposition under prototypical PWR operating conditions (pressure, temperature, and water chemistry corresponding to different burn-up points along the cycle). The effect of heat flux and crud morphology (thickness and porosity) on the rate of boron deposition will be examined using both simulated and in-situ formed crud on the cladding surface.

(b) Evaluate the effectiveness of various mitigating actions aimed at limiting the rate of boron deposition within the crud, and hence AOA, during extended cycles in high power cores.

In addition to performing hands-on experimental research on a state-of-the-art test facility, the students will be introduced to (and will perform) a wide range of quantitative analyses (EDX, SIMS, ICP-MS, and XRD). In addition to educating graduate students in nuclear engineering, the data obtained in this research is highly valuable, inasmuch as it will provide the means to validate predictive models for crud and boron deposition in high duty PWR cores.

2. EXPERIMENTAL TEST FACILITIES

2.1. OVERVIEW

The Georgia Tech AOA Test Facility allows experiments to be conducted in a pressure vessel maintained at prototypical PWR primary coolant pressure, temperature, and water chemistry conditions. Boundary conditions, i.e., the surface heat flux, water chemistry, coolant pressure and temperature, can be maintained at the desired values throughout experiments ranging from several hours to several weeks duration. Electrically-heated Zircaloy-4 test elements are immersed in the coolant for the duration of the experiments (up to several weeks each), while maintaining them at specified constant surface heat fluxes up to 5×10^5 Btu/hr-ft^2 (~1.6 MW/m^2); these heat fluxes are comparable to those present at the hot spot in a modern, high-

duty, four-loop PWR core. Initially, the facility was designed to maintain the test elements under natural convection/subcooled pool boiling conditions. The facility was later modified to allow the coolant to flow past the heated test elements at controlled velocities up to the prototypical values for PWR cores, thereby maintaining the test elements under forced convection/subcooled flow boiling conditions.

At the end of each experiment, the test elements can be rapidly isolated from the coolant by discharging the entire system coolant inventory (i.e. rapidly blowing-down the system inventory to an external tank at atmospheric pressure) and simultaneously terminating power, thereby preventing the dissolution of any boron-bearing species which may be present within the crud (including those with retrograde solubility), without causing surface burnout. Following each experiment, the test element was removed from the pressure vessel; analyses were then performed to determine the mass, thickness, composition, and overall morphology of the crud deposited on the surface, as well as the chemical composition and amount of boron-bearing species deposited within the crud. Experiments were conducted at different values of surface heat flux, exposure time (i.e. duration), pH, coolant subcooling, soluble and insoluble iron and nickel concentrations, and initial surface conditions. Early experiments utilized test elements pre-coated with a nickel ferrite layer simulating the deposited crud. For later experiments, the addition of both soluble and insoluble iron and nickel compounds promoted in-situ formation of crud with prototypical composition, thickness and morphology (porous with vapor chimneys). The remainder of this section provides a detailed description of the Georgia Tech AOA test facility and experimental test procedure. Figure 1 is a schematic of the GT-AOA Test Facility.

2.2. TEST FACILITY COMPONENTS

2.2.1. Test Loop

The test loop consists of six major subsystems: the pressure vessel, the electrodes, the mixer, the pressurizer, the blow-down system, and the let down assembly. The one gallon pressure vessel is the central component of the experiment. It is rated to a maximum pressure of 2500 psig, at a maximum temperature of 650 °F, and made of 316-stainless steel, well above the typical operating conditions of the experiment (~ 590 °F and ~ 2000 psia). The temperature within the vessel is controlled by a Watlow PID controller and can be maintained indefinitely within ±1 °F. A modulated 4000 watt heating blanket placed around the vessel exterior, and an on/off solenoid-valve-controlled cooling coil with tap water feed placed within the vessel are the control elements used to maintain the desired temperature within the vessel. The pressure within the vessel is maintained at the desired level by means of an argon gas pressurizer (to be described later). The vessel has 11 threaded ports on the bolted removable top and one threaded opening through the bottom. The top is sealed with a graphite spiral-wound gasket seal. The top threaded ports accommodate a feed line, let-down line, two electrodes, lines for the in-vessel cooling coils, a thermocouple, a rupture disk, a pressure transducer port, pressurizer port, and one spare port. The bottom of the vessel has one opening, through which the drain/blowdown line and the stirrer shaft pass. The vessel is mounted on pneumatic pistons so that it can be lowered and the inside prepared for experiments. In some experiments, a nickel screen was placed inside to match the nickel/steel area ratio for the primary system in a four-loop PWR primary system. For a typical PWR, the wetted interior components are comprised of 9.6 percent stainless steel, 65.1 percent Inconel-600, and 25.2 percent Zircaloy-4 [4], which corresponds to

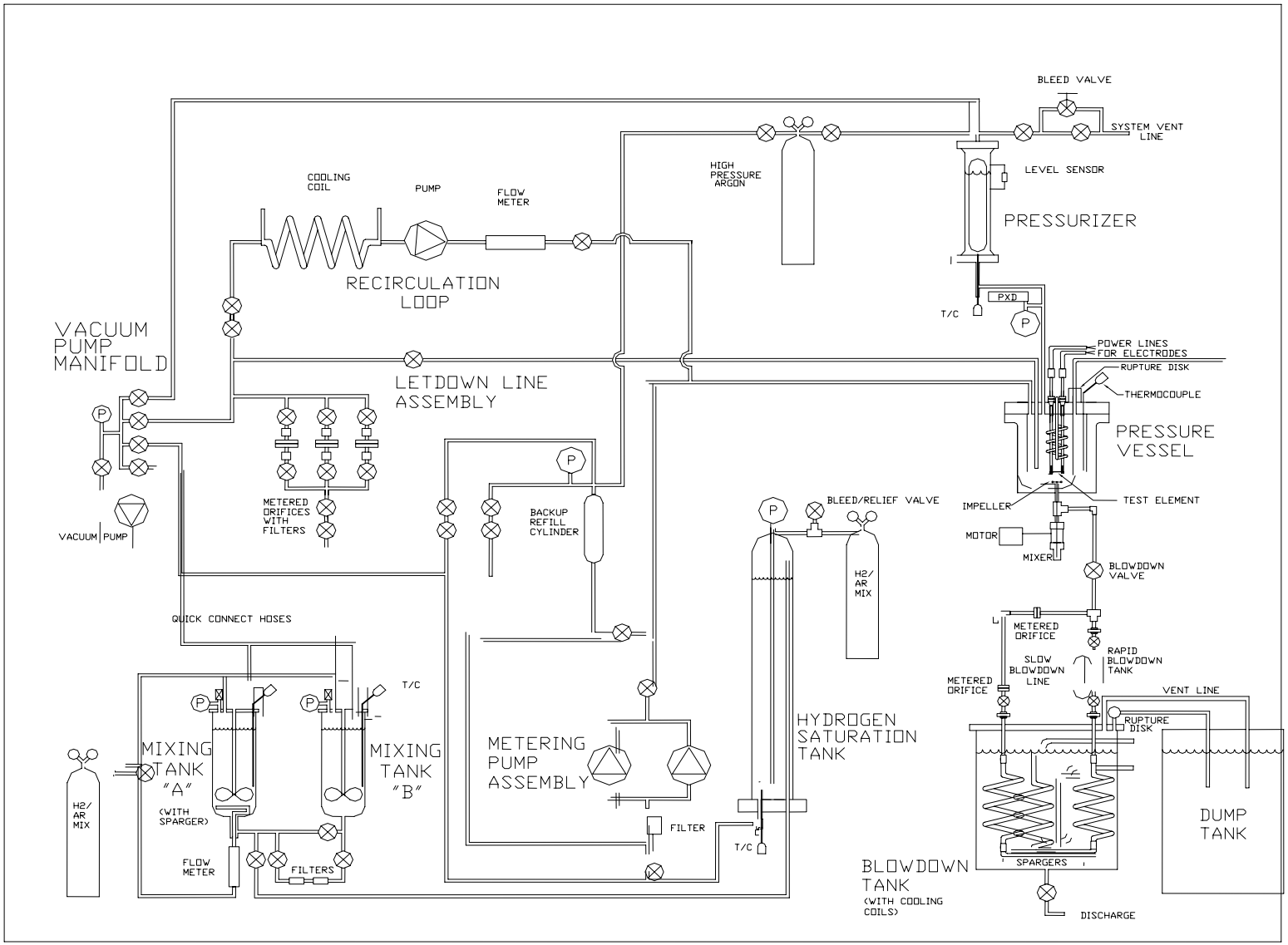

Figure 1: Schematic of the Georgia Tech AOA Test Facility.

an elemental composition of 67% nickel, 17% iron and 15% chromium (excluding the cladding). Without the nickel screen in the pressure vessel, the approximate composition for the AOA test facility is 12% nickel, 66% iron, and 17% chromium, which changes to 68%, 25% and 7%, respectively when the nickel screen is placed in the vessel. For later experiments, the addition of considerable amounts of soluble and insoluble iron and nickel compounds to simulate primary system corrosion products eliminated the need for placing the nickel screen within the vessel. The screen also represented a practical problem for vessel cleaning and elimination of carry-over crud from one experiment to the next.

The electrodes penetrate the cover of the pressure vessel and deliver a high current to the test Zircaloy test element attached to them in order to maintain the desired surface heat flux (~5×10^5 Btu/hr-ft^2). Typically, this corresponds to a current of 90 Amps. The surface heat flux also depends on the heated length of the wire, which varies slightly among experiments. The length of the electrodes has been selected so that the test wire sits approximately two-thirds of the way down in the pressure vessel. The wire shape itself has undergone some evolution as the experiment has progressed. The problem of wires breaking because of differential expansion and high contact resistance led to the final test wire design, which allows the wire to freely expand and minimizes the contact resistance between the test element and the electrodes (see Figure 2; the configurations numbers start with number two, because the first configuration was simply a straight wire). The wire holders shown in Figure 2 provide an interface between the electrodes and the wire. The wire holders are custom-made out of 316-stainless steel. The electrodes are made of stainless steel and are sealed with custom-made hybrid Teflon/Lava seals with a maximum rated temperature of 500 °F. Since this temperature is lower than the system operating temperature, the seals are located above the main body of the vessel so as to remain cooler, and a cooling fan is used to keep them below the rated temperature. The typical operating temperature for the seals during an experiment is approximately 350 °F.

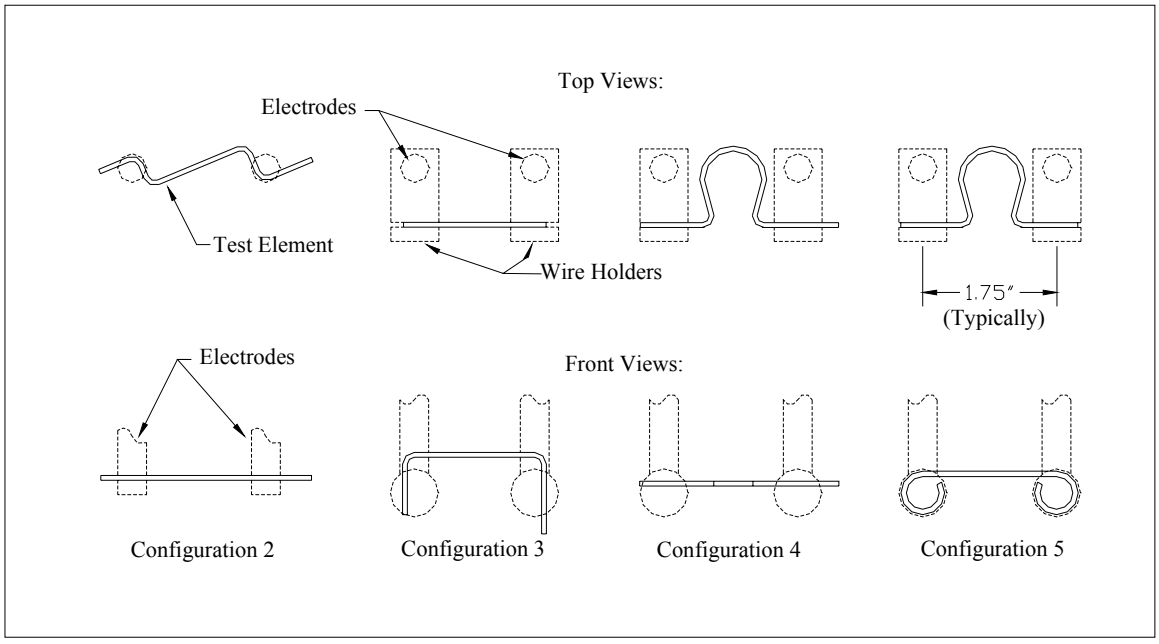

Figure 2: Diagram Showing Evolution of the Wire Configuration used in the Experiments.

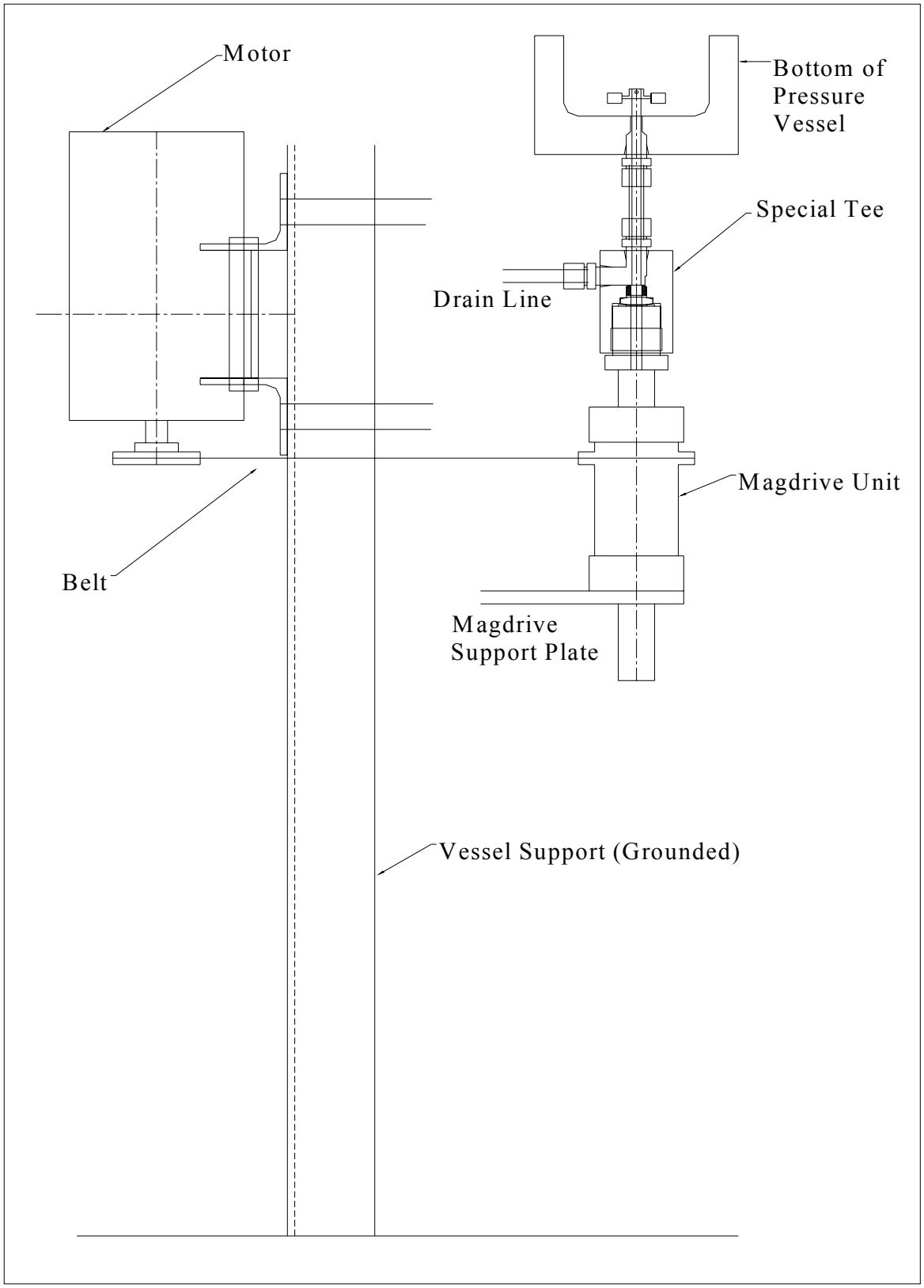

Figure 3: Schematic Diagram of the Mixing System.

The mixer provides forced coolant flow past the heated test element at controlled velocities, thereby simulating the forced convection/subcooled nucleate boiling conditions in the upper region of a high-duty PWR core. The mixer used in this experiment (MagneDrive, manufactured by Autoclave Engineers, Erie, PA) uses an external motor to drive an internal shaft coupled with permanent magnets. The internal shaft is 0.313 inches in diameter and passes through piping and into the vessel. A 2-inch diameter Rushton style impeller is mounted to the shaft and provides the agitation for the coolant. The MagneDrive unit is rated to 50,000 psig at 450 °F. The rated temperature is lower than the normal operating temperature of the pressure vessel; however, it is acceptable since the mixer is externally mounted. The motor used to drive the mixer is a Reliance Duty Master (manufactured by Reliance Electric Company, Cleveland, OH), rated to 3450 RPM at 1.5 hp, and connected to the mixer via a belt system. The motor is controlled using a ParaJust AC motor speed controller (manufactured by Parametrics, Orange, CT), which varies the power from zero percent to full power, thereby controlling the impeller speed, and hence, the coolant velocity past the heated test element. The maximum operating speed of the MagneDrive is 2000 RPM, while the typical speed during an experiment is about 800 RPM. A schematic diagram of the mixing system is shown in Figure 3. Baffles are placed in the vessel interior to prevent the coolant from simply swirling in a "rigid body" fashion. A schematic diagram of the baffles' placement within the vessel is shown in Figure 4. The baffles are arranged in a manner that forces the coolant to flow vertically upwards past the heated wire (cross flow). The stainless steel baffles are a half inch wide and mounted 90º apart on a heavy stainless steel ring. The baffle assembly is removable, so that it can be cleaned between experiments. It is oriented as shown in Figure 4, to maximize the distance from the baffles to the test wire, thereby preventing arcing between the test wire and the grounded pressure vessel.

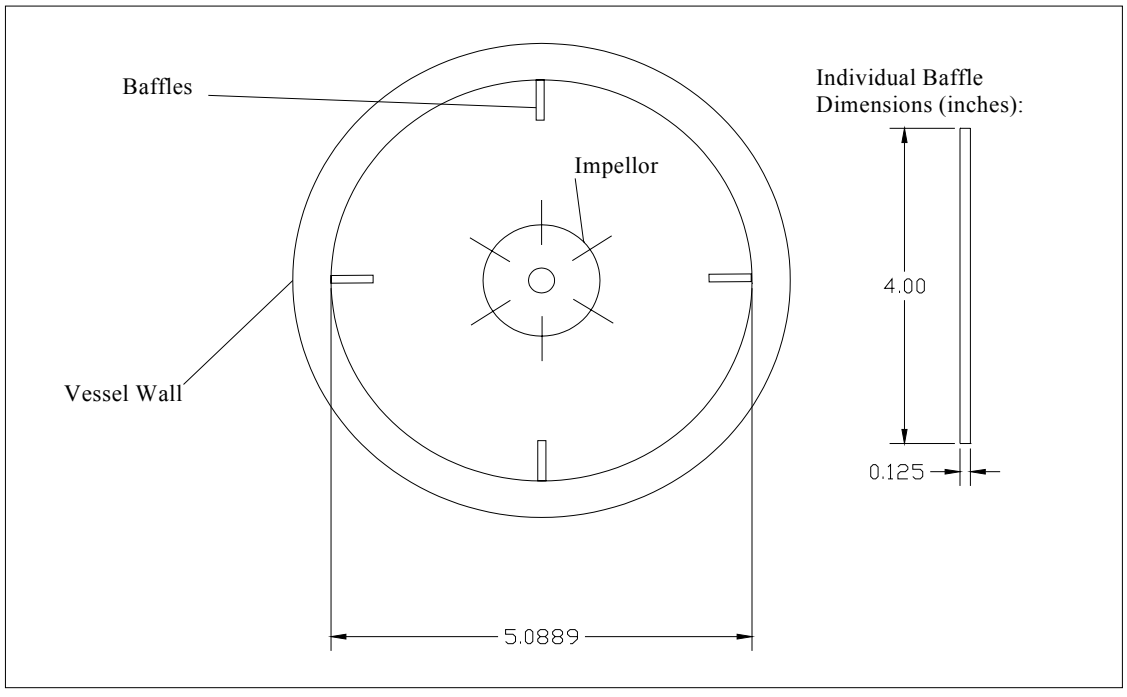

Figure 4: Baffle Configuration and Placement within the Pressure Vessel.

The pressurizer is made of 316-stainless steel and contains a hollow titanium float, an electronic level sensor, and a mechanical level indicator. The pressurizer is mounted above the pressure vessel and partially filled with liquid, so that the vessel is completely filled with liquid while a free surface is maintained within the pressurizer. The water in the pressurizer automatically compensates for any minor leaks in the system, thereby maintaining the vessel filled. The pressurizer level can be visually observed by the mechanical level indicator; variations in pressurizer level provide a direct indication of any leaks from the system. Argon from a high pressure gas cylinder (6000 psia) provides the desired system pressure within the pressurizer gas space; a precision gas regulator allows for precise control of the system pressure. With the addition of the mixer, monitoring and control of the pressurizer level becomes especially important, since the presence of a free surface within the pressure vessel itself would cause the coolant to vortex rapidly, leaving the wire bare, which would cause the test wire to instantly burnout.

The blow-down system consists of the blow-down tank, a drain line, and an isolation valve which separates the blow-down tank from the pressure vessel (Figure 1). The blow-down tank is a large low pressure, stainless steel tank in which the superheated coolant is rapidly discharged at the end of an experiment. The rapid draining of the pressure vessel necessitates a tank that can manage the high temperature coolant. The blow-down tank is rated to 100 psig and 450 ºF. Normally, it is partially-filled with water with submerged cooling coils to serve that purpose. The system coolant is discharged into the blow-down tank through a sparger placed within the tank's chilled water. The drain line connecting the blow-down tank to the pressure vessel runs through a custom stainless steel T-junction, which allows the MagneDrive mixer shaft to penetrate the vessel, while the isolation valve is either open or closed (Figure 3). The isolation valve has an extended grip so that it can be easily and rapidly opened at the end of the experiment during the rapid blow-down procedure. It is estimated that during the system blow-down, the test element becomes completely uncovered in ~ 70 ms.

The let-down assembly is designed to allow coolant samples to be withdrawn from the system during an experiment. It is also used to bleed off the coolant at the end of each experiment until the water level drops to about half an inch above the horizontal test element; at that point rapid blow-down is initiated and power input to the test element is simultaneously terminated. Three redundant lines with filters and different-sized orifices are used in case one fails during a let-down procedure. The orifice sizes are 2, 5, and 9 microns; valves are provided so that one or more letdown lines can be either individually or simultaneously used. The orifices are placed in the letdown lines so that the coolant samples can be slowly extracted. The precision gas regulator connected to the pressurizer gas space can easily maintain the system pressure during either sample extraction or slow let-down. The let-down line with the middle size orifice is normally used for sampling and excess-coolant draining, since it offers a good compromise between speed and system control. The inlet to the let-down line is placed within the pressure vessel and positioned in such a way so that its tip is slightly above the test wire. This allows all the excess coolant to be drained without uncovering the test element, so that power to the test element remains activated until the let-down process is completed and rapid blow-down is initiated through the vessel isolation valve.

2.2.2. Coolant Preparation System

The manner in which the coolant is prepared is vital to the success and reliability of the experiments. Precise control of the concentrations of various additives is necessary for maintaining the proper pH and replicating the conditions in a PWR primary coolant. System components designed solely for coolant preparation are the hydrogen saturation tank and the mixing tanks (see Figure 1). Coolant preparation begins in the mixing tanks. They are identical five gallon stainless steel tanks. Each contains a mixer operated by a top-mounted air motor. Both tanks are equipped with a heating blanket that surrounds the outside. Mixing tank "A" has a gas sparger on the bottom that bubbles argon through the coolant during mixing. The tanks can be evacuated using a vacuum pump or they can be pressurized up to 100 psig. The hydrogen saturation tank is a vertically mounted stainless steel tank maintained at a regulated pressure of 300 psig. It serves as a storage tank for the coolant and provides the means for controlling the hydrogen concentration at the desired level. The hydrogen concentration is maintained at the desired level by bubbling a hydrogen/argon (4%/96%) gas mixture through the coolant stored in the tank while maintaining the pressure at 300 psig. The hydrogen/argon mixture is used to avoid flammability concerns.

The vacuum pump (Figure 1) is used to prepare both the test loop and the coolant preparation system. It can draw a vacuum on any component in the AOA facility. It is used to remove air (i.e. oxygen) from a tank before coolant is transferred to it. The tank, whether it is one of the mixing tanks, the saturation tank, or the high-pressure vessel, is generally evacuated several times followed by argon purging, thereby significantly decreasing the concentration of oxygen. Generally, the oxygen concentration in the system is below detectable levels. The pump has an associated vacuum gauge, and a typical vacuum is approximately -27 feet of water with multiple vacuum/argon purge cycles before the tank is used.

Once the coolant is properly prepared it must be transferred to the test loop for an experiment. Two high pressure metering pumps can be used to transfer precise amounts of coolant from the hydrogen saturation tank to the high pressure vessel (see Figure 1). They are similar but not identical pumps, and are rated up to 5000 psig with a flow rate of approximately 10 mL/min. These pumps can be used at any time during the experiment, but if they were to both fail, there is a backup system that can accomplish the same goal. The coolant is transferred to an intermediate 500 mL tank from the saturation tank via a pressure differential. The tank is then isolated and brought to system pressure before transferring the liquid to the high pressure vessel. These two transfer mechanisms are used only while an experiment is in progress (to compensate for any leakage). For the initial coolant transfer before the start of the experiment, the saturation tank feeds directly into the pressure vessel at 300 psig (see experimental procedure below).

2.2.3. Data Acquisition System

The AOA test facility was instrumented with numerous sensors to monitor the various system parameters during an experiment. Readings from electronic sensors are fed through an analog to digital converter panel into a dedicated computer. A visual basic program was written that can record data at a specified interval, usually every five minutes, throughout the experiment (up to several weeks in duration). Parameters that are measured directly are the operating current,

liquid levels in the pressurizer and saturation tank, the system pressure and temperature, the Teflon electrode seal temperature, and the pressure in the saturation tank. The program uses the measured current (and voltage) to calculate the surface heat flux of the wire based on the length of the wire, which is inputted by the user at the start of the experiment. There are several other sensors in the facility used as a back up to the acquisition system described above. The pressurizer level is monitored by a mechanical level indicator that uses magnetic flaps. This sensor does not run the entire length of the pressurizer, but it can give an indication of the liquid level in the pressurizer above the half-way mark. An analog pressure gauge mounted next to the vessel provides a visual indication of system pressure. The Watlow PID controller also gives a visual reading of the vessel temperature and pressure. In addition to these manual backup sensors, pertinent data readings from the computer are recorded daily in a lab notebook as a backup to the overall data acquisition system.

2.2.4. Safety and Protection Systems

Several safety systems have been added to the facility after construction. The first is a device to mechanically prevent the electrodes from being ejected by the system high pressure in case of a Teflon/Lava seal failure. This was implemented after such a failure caused an electrode to be ejected while an experiment was in progress, which is extremely dangerous for anyone who may be in the lab. A thick Lexan shield is located directly in front of the pressure vessel while an experiment is in progress for extra protection. A narrow-range pressure relief valve was added to prevent system over-pressurization, which may lead to component damage. Specifically, the rated pressure for the titanium float in the pressurizer (~2300 psig) is well below the 2500 psig rating for the pressure vessel. During early shake-down testing of the facility, the pressurizer float had to be replaced after being crushed during a pressure transient. The narrow-range pressure relief valve is set below the rated pressure for the pressurizer float. Finally, an additional valve was installed in the vacuum manifold system, in order to isolate the vacuum gauge from the rest of the system. This gauge also had to be replaced during the initial shake-down tests after it was over-pressurized, which can happen at relatively low system pressures.

3. EXPERIMENTAL PROCEDURES

3.1. PREPARATION OF TEST FACILITY

Before the start of an experiment, the facility had to be cleaned to eliminate carry-over of corrosion products and/or contaminants from the previous run. The vessel interior is cleaned by repeatedly rinsing it with distilled water and wiping it with paper towels until no residue is left. Whenever the vessel is opened and not being worked on, a cover is placed over the bottom portion to prevent dust and other contaminants from collecting inside. The mixing tanks were also scrubbed before adding the distilled water to them to begin coolant preparation. The hydrogen saturation tank is sealed from the environment, and, therefore, did not require cleaning after each experiment. It was, however, fully evacuated and purged with argon whenever the coolant composition was to be changed. The blow-down tank contained “waste liquid” and was, therefore, only partially drained prior to each experiment. Care is taken to assure that the blow-down tank contains enough water to cover the cooling coils, in order for the cold water within

the tank to facilitate condensation during rapid blow-down of the test facility upon conclusion of an experiment. Partial draining of the blow-down tank is achieved through a drain line at the bottom of the tank. The other major components requiring cleaning are those that interact with the wire. Great care is taken to clean the electrical contacts for the wire. The contact points of the wire holders must be removed of all tarnish and deposits from previous experiments so that arcing is less likely to occur. This is also important to reduce the contact resistance as much as possible so that the heat flux calculation will be accurate for the portion of the wire that is expected to receive the most crud deposition. An arc from the electrodes to any part of the wire will cause intense localized heating and vaporization of the surrounding coolant. This, in turn, may cause the wire to fail, thereby producing no reliable results from the experiment. The baffles and impeller surfaces are cleaned prior to each experiment; they are removed from the pressure vessel for this purpose and reinstalled after they are cleaned.

3.2. COOLANT PREPARATION

A fresh batch of coolant was prepared prior to each experimental run with generally eight or twelve liters prepared. Distilled water was carefully weighed and placed into mixing tank "A" (see Figure 1). The water was then forced through a series of filters into tank B. The filters removed particulate matter down to one-half micron. The water was filtered a second time as it was transferred from tank B back into tank A.

Tank A was stirred continuously and heated to approximately 200^{o}F. Argon was bubbled through the water using a gas sparger to remove oxygen. Periodically, a vacuum was pulled on the tank to remove gas above the surface of the water and to promote boiling of the water.

After several hours of heating and degassing, boric acid crystals were added to achieve the desired boron concentration (usually 1500 wppm). Early experiments used reagent grade boric acid that met or exceeded purity specifications for boric acid used in PWR plants. Later experiments used ultra-pure (99.9995%) boric acid crystals in an effort to reduce contaminants. A measured amount of lithium hydroxide solution was added to achieve the desired pH_T value (generally a lithium concentration of 3.47 wppm was used, but higher concentrations were used in some experiments to either increase the pH or compensate for the effect of added soluble corrosion products). In some experiments, soluble corrosion products (iron and nickel compounds) were added to the water to promote crud deposition on the test wire during the relatively-short exposure time of the experiment (few weeks versus a few months in an actual PWR core). Soluble nickel and iron nitrates and insoluble nickel ferrite were used for that purpose. The insoluble nickel ferrite was not added to the coolant in the mixing tanks; instead the appropriate amount was weighed and placed in a dispersion device directly within the pressure vessel (secured by a nickel wire and positioned approximately 2 cm above the test element). After adding the soluble chemicals to achieve the desired concentrations, the mixing tank was closed and mixing and degassing continued for several more hours. The mixing and degassing process took nearly six to eight hours to complete.

While mixing and degassing took place in tank A, the hydrogen saturation tank was prepared to receive the coolant. First, it was emptied of all liquid and then evacuated using the vacuum pump. The tank was purged with a 4% hydrogen/96% argon mixture and again evacuated. This

was repeated a third time, and then filled with hydrogen/argon at about 30 PSIG. The use of a hydrogen/argon mixture was necessitated by flammability concerns.

When mixing and degassing was completed, all of the coolant was transferred to the hydrogen saturation tank by pressurizing tank A with argon at 50 psig. More hydrogen/argon gas was then introduced into the saturation tank until the pressure reached 300 psig. This gas mixture was continuously fed to the bottom of the tank and bubbled up through the coolant. Gas was allowed to escape from the top of the tank through a metering bleed valve. Pressure within the tank was maintained at 300 psig, and gas bubbled through the coolant for the duration of the experiment. The pressure of 300 psig was used to ensure the proper (prototypical) concentration of dissolved hydrogen in the coolant was maintained. The coolant was saturated with hydrogen for a minimum of 24 hours to achieve the desired concentration before it was used in an experimental run.

3.3. TEST ELEMENTS

The test elements used in the experiments are 0.0625 inch diameter wires made of Zircaloy-4, the same material used for cladding fuel rods in many PWR cores; other cladding materials (e.g. Zirlo) were not available in the desired form. The wire was mounted between electrodes in the pressure vessel and resistively heated by passing a large current through it. A new test element was used in each experiment.

Early experiments indicated that pre-conditioning the wires either by oxidation or deposition of a thin nickel ferrite coating promoted more rapid growth of a crud layer. This is important since in-situ formation of crud in a PWR typically takes several months or more, while the experiments are expected to last only a few weeks each. The wire surface was pre-oxidized by baking it in an air atmosphere for 12 hours at 675 ^{o}F. This process proved successful; coupled with the addition of soluble and insoluble corrosion products in the coolant, it was possible to accelerate crud deposition on the wire by more than an order of magnitude. Crud layers with prototypical composition and morphology (porous with chimneys) were routinely formed in many experiments conducted during this investigation; some experiments produced even thicker crud layers than those observed in high duty plants experiencing AOA. Previous experiments used Zircaloy-4 wires pre-conditioned by either deposition of a nickel ferrite coating or coating using spray pyrolysis. Details of the spray pyrolysis process and the characteristics of the pre-deposited nickel ferrite layers can be found in Appendix A. For the experiments conducted during the last two years of this investigation, all crud deposits on the wire were formed in-situ. The wires were bent into a horseshoe shape with flattened loops on each end. This shape gives the wire greater flexibility to handle differential thermal expansion between the wire and the electrodes holding it. The flattened loops create a much greater contact area between the wire and electrodes and reduce incidents of arcing (see Figure 2).

3.4. CONDUCT OF A TYPICAL EXPERIMENT

The general procedure for the conduct of experiments is as follows. While the coolant is prepared as described in section 3.2, the pressure vessel is cleaned and rinsed with distilled water to remove residual contaminants from the previous test run. Prior to installation, the Zircaloy-4

test is weighed to within 10 micrograms in a high-precision Sartorius balance. The wire is attached to the electrodes in the pressure vessel; insoluble corrosion products (nickel ferrite), if any are to be used, are then placed in a porous dispersion device within the vessel before sealing the pressure vessel. Air is evacuated from the pressure vessel and all the piping using the vacuum pump. The system is then purged with argon. Evacuation and purging is repeated two more times to remove air (i.e. oxygen) from the system.

Next, the coolant is transferred from the hydrogen saturation tank to the pressure vessel and pressurizer. This is accomplished by filling the vessel with argon to a pressure of 200 psia before connecting it to the hydrogen saturation tank. Coolant transfer from the hydrogen saturation tank to the vessel and pressurizer continues until the pressurizer is nearly one third full (pressurizer level indication is first observed at that point). The heating blanket around the pressure vessel is turned on; over the next several hours the temperature in the pressure vessel is ramped up to the desired operating temperature, where it is held constant to within +/- 1 ^{o}F. The desired operating pressure within the system is maintained by supplying argon to the pressurizer from the high-pressure gas cylinder equipped with a precision regulator. Coolant is slowly bled from the system as it expands during the heat-up process in order to control the level in the pressurizer. The pressurizer level during the heat-up period is usually maintained between 60% and 90%. During the heat-up period, nearly 600 mL of liquid are discharged through the middle-sized orifice let-down line. After the system reaches thermal equilibrium, and the desired inventory, i.e. pressurizer level (typically 90%) is attained, the stirrer is turned on and the impeller rotational speed is adjusted to the desired value. Alternating current supplied to the test element is slowly ramped up until the desired heat flux is reached. The data acquisition program is started and is set to record 20 channels of data from the system at five-minute intervals for the duration of the experiment.

When an experiment is scheduled to be terminated through rapid blowdown of the pressure vessel, coolant is slowly bled from the pressure vessel at the conclusion of the test period through one or more of the three let-down lines until the coolant level is approximately one centimeter above the test element. Pressure and temperature, as well as heat flux, are held constant at normal operating conditions during the several hours it takes to reduce the coolant level to that point.

To initiate blowdown, power to the test element is suddenly cut off. At the same moment, the large isolation valve is opened. The very high pressure in the pressure vessel (approximately 2000 psig) rapidly forces the remaining hot coolant out of the vessel and into the chilled blow down tank. Using this procedure, the test element is rapidly (<70 milliseconds) isolated from the coolant to prevent dissolution of any boron-bearing material (including those with retrograde solubility, such as $LiBO_2$) which may be present in the crud. After the rapid blowdown, argon is bled into the system to reduce oxidation as the pressure vessel cools from nearly 600 ^{o}F to room temperature. When cool, the pressure vessel is opened and the test element is removed.

After an experiment, the test element is examined to verify the presence or absence of boron-bearing compounds and quantify the amount of boron deposition using a number of different methods (SEM/EDX; SIMS; XRD; ICP-MS). Coolant samples collected during the experiment are also analyzed.

4. RESULTS

A total of 48 experiments ranging in duration from one to sixty one days have been conducted during the course of this investigation. Table 1 lists the experimental conditions for each experiment; these include: (a) the wire configuration (number corresponds to those shown in Figure 2); (b) the initial surface condition of the wire (bare or pre-coated); (c) the average surface heat flux during the experiment (typically 4.0 to 5.0 $\times$ 10^5 Btu/hr-ft^2); (d) the test duration in days; (e) the coolant conditions at the beginning of the experiment (boron, lithium, soluble nickel, and soluble iron concentrations, along with the amount, if any, of nickel ferrite added directly to the pressure vessel); and (f) whether or not the mixer was activated (forced versus natural convection conditions). Table 2 summarizes the outcome of the experiments; among the parameters included are: (a) the weight gain during the experiment; (b) the calculated average thickness of the crud layer (assuming 50% porosity and a solid density of 4.3 g/cc corresponding to nickel ferrite); (c) measured crud layer thickness (differs from calculated thickness because of deviations from the assumed porosity and composition); (d) an indication as to whether or not the wire broke during the experiment; and (e) indications as to whether XRD and/or ICP-MS analyses were performed following the experiment. In all cases, SEM/EDX analyses were performed.

The first twenty experiments listed in Tables 1 and 2 are relatively short in duration (< 2 weeks); they can be viewed as "shake-down experiments" aimed at optimizing the test facility. Among the first problems eliminated was the formation of contaminant-based crud on the heated surface. The largest source of contamination was the Lava electrode seals, which allowed large quantities of calcium to leach out into the coolant and eventually deposit on the heated test element. The problem was solved by replacing the Lava seals with custom designed hybrid Teflon/Lava seals. Another large source of contamination was the electrodes themselves. The electrodes were originally made from nickel-plated copper rods. The nickel plating eroded after several experiments, which led to the release of copper into the coolant. This problem was eliminated by replacing the electrodes with custom electrodes made entirely from stainless steel.

Some of the early experiments (#3, 4, 8, 12 and 25) used wires pre-coated with a layer of porous nickel ferrite. The coatings were applied by Dominion Engineering of Washington, DC. These coatings, however, proved to be fragile; they generally did not survive the rapid blow-down process at the conclusion of the experiments, and were, therefore, discontinued. Other earlier experiments (#29 and 30) used pre-coated wires prepared using the spray pyrolysis process (see Appendix A). This process proved to be cumbersome and did not produce the robust crud needed for the test conditions used in this study. The procedures used in experiments #31 through 48 which led to in-situ formation of prototypical crud proved to be successful and reliable, and were, therefore, used in all later experiments. The thickness of the crud layer formed in-situ during experiments conducted during those experiments ranges from a low of 8 microns to a high of nearly 350 microns, which exceeds the crud thickness values observed in AOA plants. These results indicate the effectiveness of the method used in this investigation to form prototypical crud at an accelerated rate by adding soluble and insoluble nickel and iron compounds to the coolant. The results also indicate that crud deposition can be significantly retarded by adjusting the water chemistry conditions despite the presence of high levels of simulated corrosion products.

Table 1: Starting conditions of all experiments.

#	ID	Wire shape	Pre-coated Wire	Heat Flux (kBtu/hr-ft^2)	days	Coolant Composition (B wppm; Li wppm; Fe wppm; Ni wppm & g of $NiFe_2O_4$)*					Mixer
48	0523 0606 05	5	Bare	505	14	1500	5.6	20	10	0.2	Yes
47	0331 0401 05	5	Bare	505	1	1500	5.6	20	10	0.2	Yes
46	0303 0317 05	5	Bare	505	14	1500	5.6	20	10	0.2	Yes
45	0216 0302 05	5	Bare	510	14	1500	5.6	20	10	0.2	Yes
44	1209 1223 04	5	Bare	475	14	1500	5.6	20	10	0.2	Yes
43	1102 1207 04	5	Bare	475	35	1500	5.6	20	10	0.2	Yes
42	1028 1029 04	5	Bare	460	1	1500	5.6	20	10	0.2	Yes
41	0917 1022 04	5	Bare	480	34	1500	5.6	20	10	0.2	Yes
40	0908 0916 04	5	Bare	480	7	1500	5.6	20	10	0.2	Yes
39	0804 0903 04	5	Bare	480	30	1500	3.3	20	10	0.2	Yes
38	0624 0729 04	5	Bare	480	34	1500	3.1			0.2	Yes
37	0513 0617 04	5	Bare	495	34	1500	5.6	20	10		Yes
36	0504 0511 04	5	Bare	490	7	1500	5.6	20	10		Yes
35	0326 0430 04	5	Bare	460	34	1500	5.6	20	10	0.2	Yes
34	0218 0319 04	5	Bare	470	30	1500	5.6	12	6.3		Yes
33	0912 1015 03	5	Bare	450	33	1500	5.6	12	6.3		-
32	0801 0902 03	5	Bare	470	33	1500	5.6	12	6.3		-
31	0527 0630 03	5	Bare	415	34	1500	5.6	20	5		-
30	0328 0414 03	5	Yes	445	17	1500	5.6	20	5		-
29	0313 0324 03	5	Yes	455	11	1500	5.6	20	5		-
28	1219 0128 03	5	Bare	430	40	1500	5.6	12	12.6		-
27	1031 1203 02	5	Bare	445	33	1500	5.6	12	12.6		-
26	0819 0916 02	5	Bare	430	28	1500	5.6	12	12.6		-
25	0628 0726 02	3	Yes	375	28	1500	3.97				-
24	0423 0624 02	5	Bare	400	61	1500	3.97			1.7	-
23	0306 0418 02	5	Bare	500	43	1500	3.47			0.9	-
22	0207 0227 02	5	Bare	500	20	1500	3.47			~1	-
21	0117 0130 02	5	Bare	400	14	1500	3.47	0.2	0.2	&	-
20	1017 1029 01	4	Bare	350	12	1500	3.47	0.2	0.2	&	-
19	1001 1008 01	4	Bare	420	7	1500	3.47	0.2	0.2	&	-
18	0911 0920 01	4	Bare	400	8			0.1	0.1	&	-
17	0822 0829 01	4	Bare	450	7						-
16	0808 0813 01	4	Bare	600	5						-
15	0802 0807 01	3	Bare	350	5						-
14	0731 0731 01	3	Bare	400	<1						-
13	0618 0625 01	3	Bare	400	7						-
12	0530 0611 01	2	Yes	300	12	1500	3.47	0.05	0.05	&	-
11	0504 0514 01	2	Bare	440	10	1500	3.47	0.05	0.05	&	-
10	0419 0501 01	2	Bare	425	12	1500	3.47	0.05	0.05	&	-
9	0328 0409 01	2	Bare	450	12	1500	1.71				-
8	0321 0323 01	2	Yes	440	2	1500	3.47				-
7	0307 0319 01	2	Bare	450	12	1500	3.47				-
6	0221 0305 01	2	Bare	450	12	1500	3.47				-

5	0201 0211 01	2	Bare	400	10	1500	3.47				-
4	0119 0128 01	1	Yes	400	9	1500	3.47				-
3	0104 0115 01	1	Yes	300	11	1500	3.47				-
2	1227 0102 01	1	Bare	300	6	1500	3.47				-
1	1215 1216 00	1	Yes	500	1	1500	3.47				-

[&] Nickel is in the form of $NiSO_4$ and iron is in the form of $FeCl_3$ was used for these experiments

Prototypical crud formation is important to assure applicability of this research to operating reactors. As mentioned earlier, the presence of contaminants in the crud was significantly reduced, thereby increasing the iron and nickel fractions in the crud to prototypical levels. This is illustrated in Figure 5 below, which includes values of the nickel and iron concentrations in the crud obtained from the EDX data. The majority of the crud mass produced in later experiments was primarily iron and nickel as opposed to the contaminant-based crud produced in earlier experiments. In addition to the need for a prototypical composition, it is important for the crud to have the correct morphology necessary to concentrate and deposit the boron-bearing species, i.e. a porous layer with chimneys. Examples of porous crud formed in-situ during this study are shown in Figures 6 and 7.

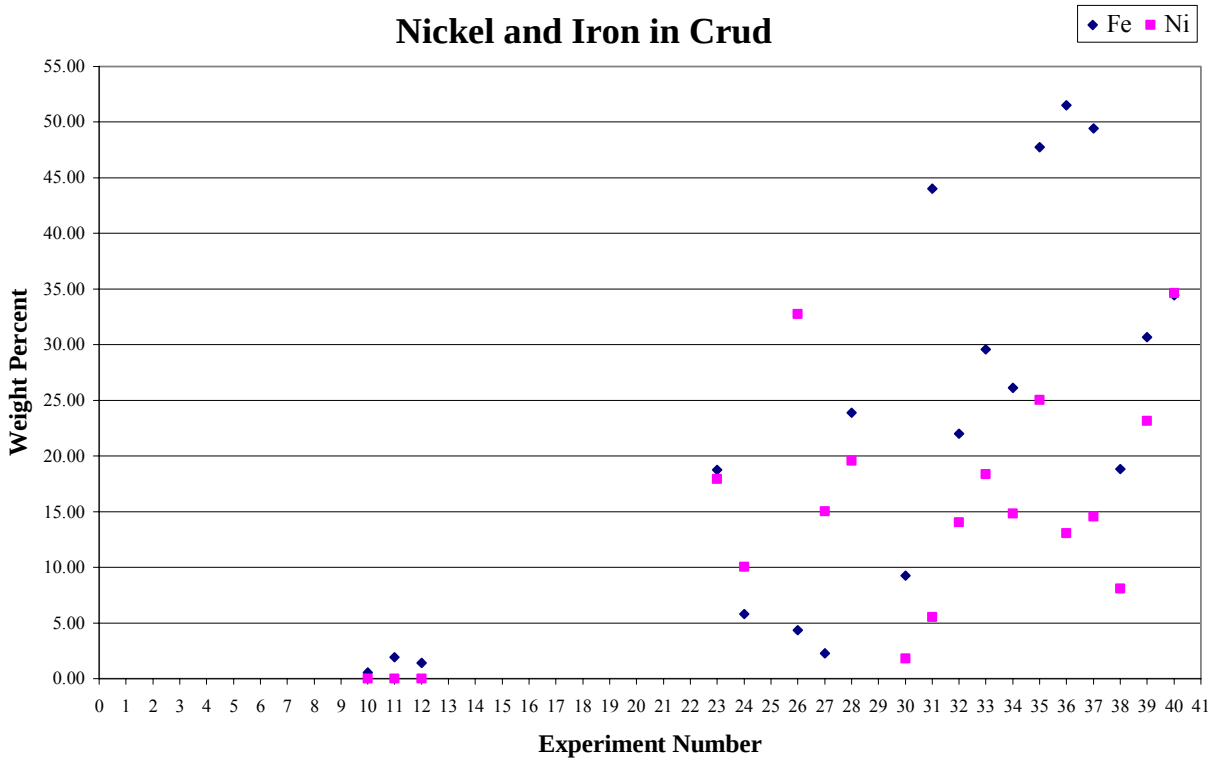

Figure 5: Nickel and Iron Concentrations in Experimental Crud by Experiment Number.

Table 2: Result Summary of All Experiments.

#	ID	Duration (Days)	Weight Gain (mg)	Wire Broke?	Other Notes	Thickness (μm)*	Thickness(μm)+	ICP-MS	XRD
48	0523 0606 05	14	275.9		Pressure=2200 psia	237.7	275.9		
47	0331 0401 05	1	73		Large leakage	69.3	106		
46	0303 0317 05	14	266		Pressure=1800 psia	230.1	178		Y
45	0216 0302 05	14	210		Pressure=1800 psia	186.4			Y
44	1209 1223 04	14	232	-		203			
43	1102 1207 04	35	259	-		225			
42	1028 1029 04	1	90	Y		85			
41	0917 1022 04	34	231	-		203			Y
40	0908 0916 04	7	90	Y	Power transient due to outage	85			
39	0804 0903 04	28	386	-		318			Y
38	0624 0729 04	34	6	-		6			
37	0513 0617 04	34	40	-		39		Y	Y
36	0504 0511 04	7	20	-	Leakage & unusual current behavior	20		Y	
35	0326 0430 04	34	435	-		352		Y	Y
34	0218 0319 04	30	11	-		11		Y	
33	0912 1015 03	33	8	-		8			
32	0801 0902 03	33	-3	Y	No heat flux for one day before blow-down				
31	0527 0630 03	34	25	-		25		Y	
30	0328 0414 03	17	167	Y	No heat flux for 3 days before blow-down	151		Y	
29	0313 0324 03	11	125	Y	No heat flux for 3 days before blow-down	116		Y	Y
28	1219 0128 03	40	214	-		190		Y	Y
27	1031 1203 02	33	-	-					
26	0819 0916 02	28	31	-		30			
25	0628 0726 02	28	-14	-	Pre-coating came off				
24	0423 0624 02	61	7	-		7		Y	
23	0306 0418 02	43	48	-		46.4			
22	0207 0227 02	20	6	-		6			
21	0117 0130 02	14		-	Hybrid electrode seals first used				
20	1017 1029 01	12	-	-					
19	1001 1008 01	7		Y	No heat flux for one day before blow-down				
18	0911 0920 01	8		Y	No heat flux for one day before blow-down				

17	0822 0829 01	7		Y	Electrode seal failure				
16	0808 0813 01	5		Y	No heat flux for 2 days before blow-down				
15	0802 0807 01	5		Y					
14	0731 0731 01	<1		Y	Wire broke immediately				
13	0618 0625 01	7		Y	Large vessel leakage				
12	0530 0611 01	12	18	-	Pre-coating came off				
11	0504 0514 01	10	17	-	Slow cool-down				
10	0419 0501 01	12	30	-					
9	0328 0409 01	12	43	-					
8	0321 0323 01	2	-	Y	Pre-coating came off				
7	0307 0319 01	12	48	-					
6	0221 0305 01	12	32	-	Slow cool-down				
5	0201 0211 01	10	50	-	Slow cool-down				
4	0119 0128 01	9		Y	Pre-coating came off, 2 days no heat flux				
3	0104 0115 01	11	-43	-	Pre-coating came off				
2	1227 0102 01	6		-	Failure in rapid blow-down				
1	1215 1216 00	1		Y					

***** Thickness here is the calculated thickness, assuming 50 % porosity and density of 4.3 g/cc corresponding to nickel ferrite.

+ Measured thickness (limited data available only for later experiments)

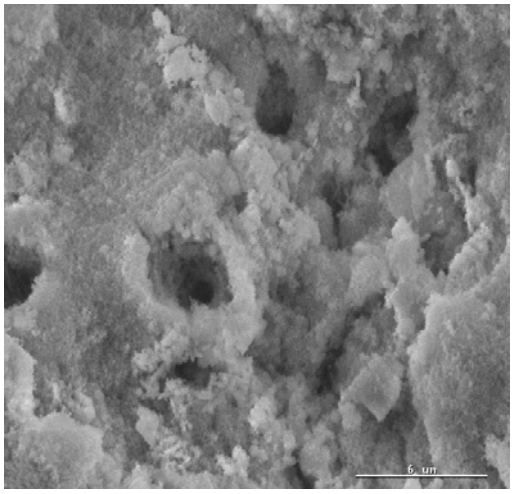

Figure 6: Crud from Experiment # 39 (4000x magnification)

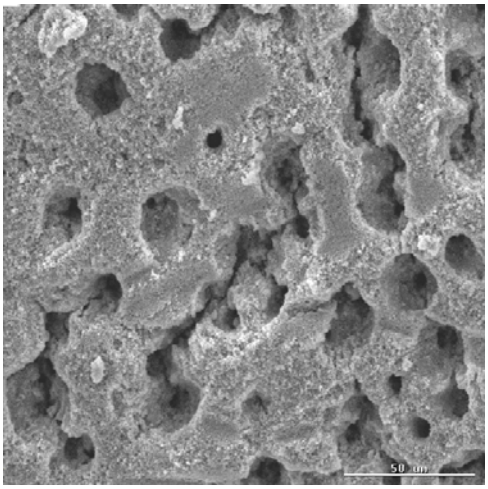

Figure 7: Crud from Experiment #36 (500x magnification)

The nickel-to-iron ratio in the crud is another important parameter used to characterize the crud composition. Plant data shows significant differences in the nickel-to-iron ratios within the crud among plants with different AOA severities; plants with severe AOA have higher nickel-to-iron ratios in the crud. The crud deposited in this study appears to follow that trend, inasmuch as the nickel-to-iron ratio varies among experiments depending on the amount of boron deposition within the crud. Figure 8 shows a plot of nickel-to-iron ratio against deposited boron weight percent. The numerical values used to produce this graph were obtained by averaging the concentration values measured using EDX and ICP-MS. The figure shows that experiments/crud samples with significantly less than one percent boron deposition all have a nickel to iron ratio around 0.5 or less. The one exception is the crud from experiment #40 which underwent a slow cool-down at end the experiment instead of a rapid blow-down. In that case, it is expected that the boron species with retrograde solubility would go back into the coolant as apparently happens in a PWR core. Using this rationalization, the crud formed under AOA conditions should (and in that case does) have a higher nickel-to-iron ratio and little or no boron (because of the retrograde solubility of the deposited boron species). Crud samples with more than one percent boron by weight have more variance in the nickel to iron ratio, but the general increasing trend is evident.

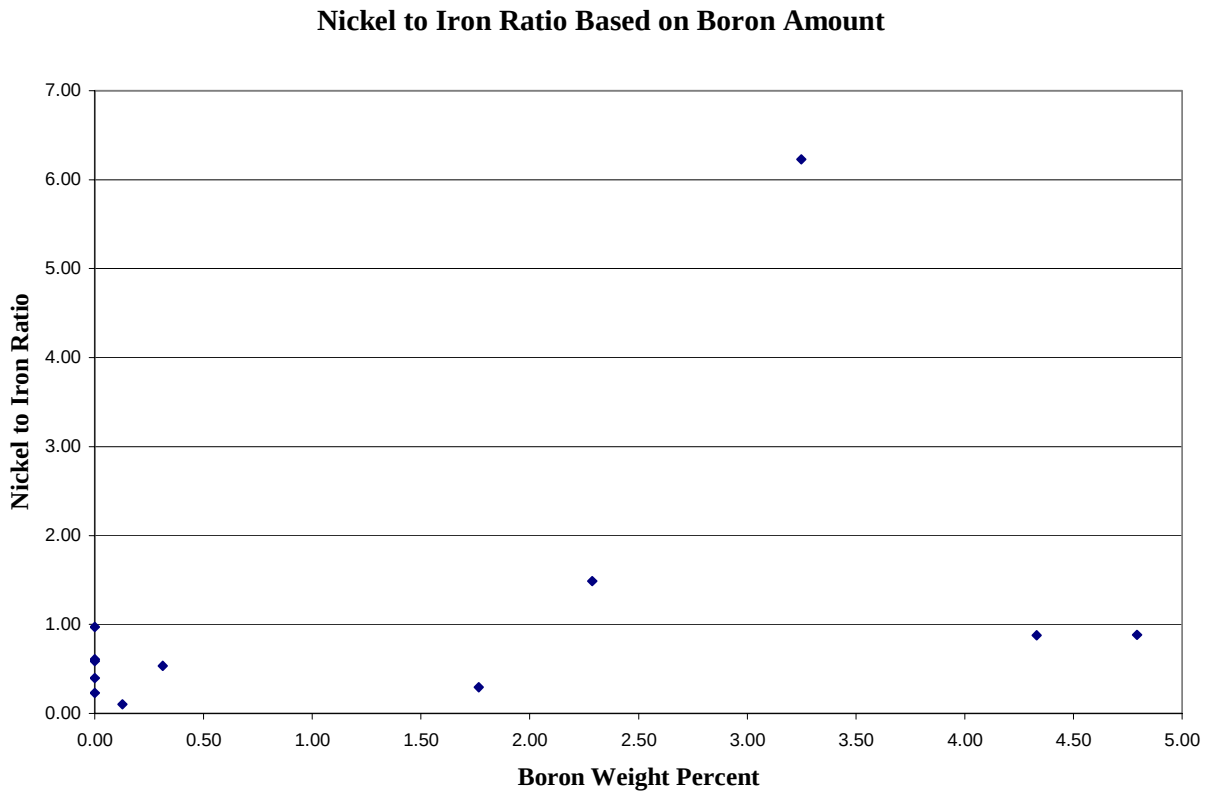

Figure 8: Relationship between Amount of Boron Deposition and Crud Nickel-to-Iron Ratio.

Among the important results obtained in this investigation is the capture and identification of the boron-bearing species in the crud. The presence of boron in the crud indicates that the rapid-blowdown procedure used in this experiment can readily capture the boron-bearing species which may be present in the crud, including those with retrograde solubility. X-ray diffraction was used to identify the chemical species of the deposited boron-bearing material. Experiment #35 was conducted under ideal conditions for crud growth. Both particulate and soluble iron and nickel were added to the coolant to accelerate crud growth; the experiment was conducted with a target pH of 7.1. This led to a crud deposition of 435 mg of mostly nickel and iron species on the Zircaloy-4 test wire, which corresponds to 8300 mg/dm^2. This crud deposit had large crystals scattered throughout as shown in Figures 9 and 10. EDX analyses of the crystals produced an average boron concentration of 14.5 weight percent. X-ray diffraction of scraped crud from this experiment showed the presence nickel ferrite, iron oxide, lithium iron nickel oxide, and most importantly, lithium tetra borate $Li_2B_4O_7$, which produced the highest peak in the diffraction pattern (Figure 11). The mineral name for lithium tetra borate is diomignite. To the best of our knowledge, this is the first time that the boron-bearing species associated with AOA has been captured and unambiguously identified. This result is consistent with earlier SIMS data obtained at Georgia Tech which suggested that the lithium-to-boron ratio in the deposited species is less than unity, thereby contradicting the lithium metaborate ($LiBO_2$) hypothesis commonly inferred by industry [4].

Lithium tetra borate crystals are commonly studied because of their piezoelectric applications. Different methods have been studied in order to improve the structural qualities of the crystals and grow them more economically. Among the methods reported in the literature is the hydrothermal growth technique, in which crystals are grown in an aqueous environment under elevated temperature and pressure. Ideal temperature and pressure conditions for hydrothermal growth of lithium tetraborate have been reported as 482 °F and 1450 psia, respectively [5]. The materials necessary for this process are boric acid and lithium hydroxide [6]; consistent with the conditions and coolant composition in a PWR core. This may explain how the crystals are able to grow in some of our experiments, and may explain how they grow in PWRs as well.

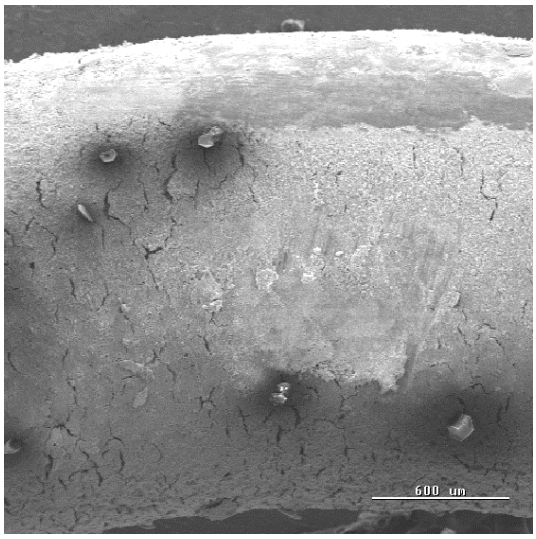

Figure 9: SEM Image of Crud from Experiment #35 (40x Mag).

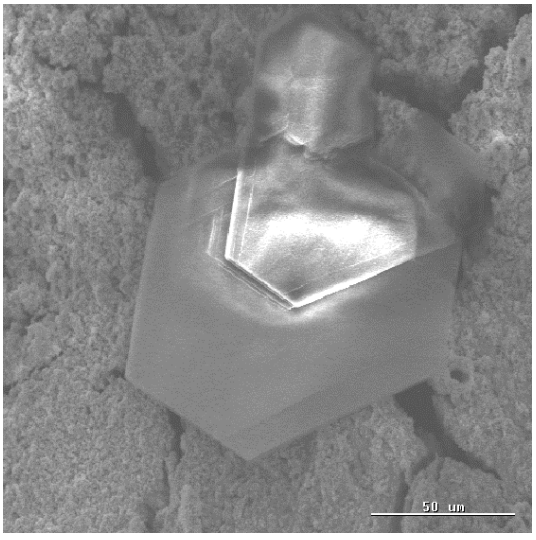

Figure 10: SEM Image of a Crystal from Expt #35 (500x Mag).

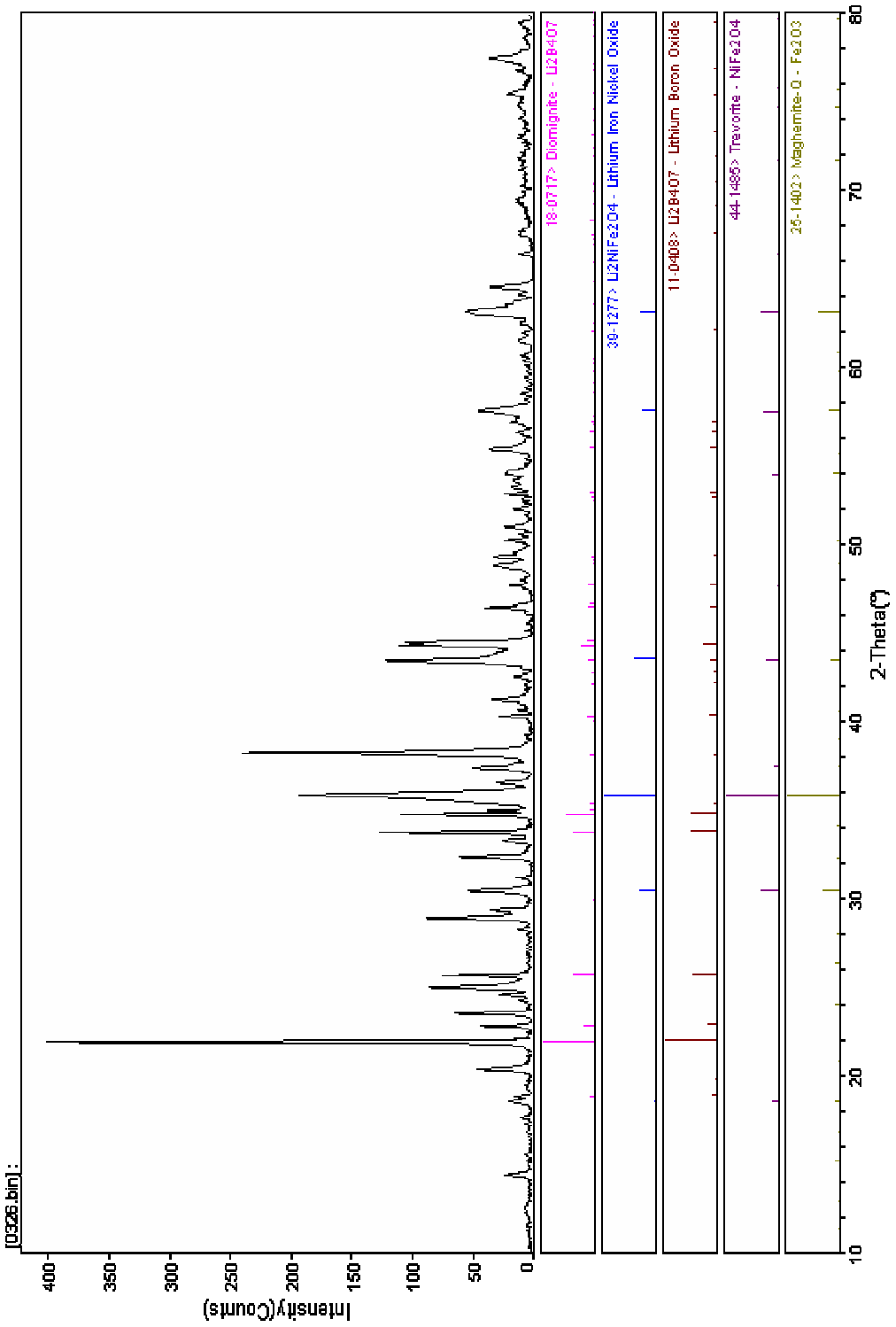

Figure 10: X-Ray Diffraction Pattern for Crud from Experiment #35.

The experiments conducted in this investigation provide guidance on the effect of various parameters on crud growth, and hence, boron deposition. The coolant pH has a significant effect on crud growth. Results found in this experiment confirm what has been suggested for the industry in that a higher pH will result in less crud growth, and hence, boron deposition. The one experiment that most prominently displays the high pH effect is Experiment #24. This experiment was operated for nearly 50% longer duration (61 days) and had nearly twice the amount of simulated corrosion products (nickel ferrite) used in experiment #23, yet produced only a fraction of the crud obtained in experiment #23. Since no soluble iron was added to these two experiments, the coolant pH is known with a high level of confidence. Other experiments also support the general pH trend, although the exact value of the pH is uncertain because of the iron nitrate addition. The three high pH experiments (#32 through 34) have less crud than the one comparable low pH experiment (# 31) even though they had a much higher heat flux (i.e. more subcooled boiling). There was one deliberate low pH experiment that showed a very large crud deposit (#39); the target pH for that experiment was 6.6. Significant crud deposition was observed during that experiment.

5. CONCLUSIONS

A total of forty eight experiments ranging in duration from one day to nearly two months have been conducted in a pressure vessel at prototypical PWR primary coolant pressures and temperatures corresponding to core regions experiencing AOA. The concentrations of boron, lithium, hydrogen, and oxygen in the coolant were controlled and maintained at prototypical PWR values corresponding to beginning-of-cycle conditions. Electrically-heated Zircaloy-4 test elements were immersed in the coolant for the duration of the experiments (up to sixty one days), while maintaining them at specified constant surface heat fluxes up to 5×10^5 Btu/hr-ft^2 (~1.6 MW/m^2); these heat fluxes are comparable to those present at the hot spot in a modern, high-duty, four-loop PWR core. Nearly one third of the experiments were conducted while the coolant was forced to flow past the heated surface (forced convection/subcooled flow boiling), while the remaining experiments were conducted under natural convection/subcooled pool boiling conditions. In nearly two-thirds of the experiments, soluble and insoluble corrosion products (iron and nickel compounds) were added to the coolant in order to accelerate in-situ crud deposition (few weeks versus few months for actual PWR cores).

At the end of each experiment, the test elements were rapidly isolated from the coolant by discharging the entire system coolant inventory (i.e. rapidly blowing-down the system inventory to an external tank at atmospheric pressure) and simultaneously terminating power, thereby preventing the dissolution of any boron-bearing species which may be present within the crud, without causing surface burnout. Following each experiment, the test element was removed from the pressure vessel; analyses were then performed to determine the mass, thickness, composition, and overall morphology of the crud deposited on the surface, as well as the chemical composition and amount of boron-bearing species deposited within the crud. Experiments were conducted at different values of surface heat flux, exposure time, pH, coolant subcooling, soluble and insoluble iron and nickel concentrations, and initial surface conditions. Early experiments utilized test elements pre-coated with a nickel ferrite layer simulating the deposited crud. For later experiments, the addition of both soluble and insoluble iron and nickel compounds promoted in-situ formation of crud; crud with prototypical composition, thickness,

and morphology was consistently formed in those experiments. Upon conclusion of each experiment, analyses were performed to identify the boron hideout species, verify the presence or absence of lithium metaborate, and quantify the amount of boron-bearing material deposited within the crud.

The data obtained in this research indicate that the experimental technique used in this investigation can be successfully used to form PWR crud with prototypical composition and morphology, and that the boron-bearing species deposited in the crud can be successfully captured using the rapid blow-down technique. Significant amounts of boron were deposited in many experiments with in-situ formed crud; analyses of these deposits indicate that lithium tetra-borate, $Li_2B_4O_7$ (Diomignite), may be the dominant boron deposition species. This result is consistent with earlier work performed at Georgia Tech which suggests that the lithium-to-boron ratio in the deposited boron species is less than unity (i.e. less than the value for lithium metaborate) [4]. The data also suggest that operation at moderately elevated pH (~ 7.7) can significantly retard crud and boron deposition. This result is consistent with recent suggestions by industry to increase the pH levels for operating PWRs.

The quantitative data obtained in this investigation can be used to verify the validity of proposed mechanistic models for crud and boron deposition; these models can then be incorporated within mass-balance-based AOA assessment codes such as the BOA code widely used by industry [3]. In addition to the experimental data obtained during this investigation, this research has been used to train and educate students in areas of direct engineering interest to the nuclear power industry, including reactor operations, thermal-hydraulics, reactor chemistry, and core physics. The research offered students the opportunity to utilize state-of-the-art analytical techniques such as EDX, XRD, SIMS, and ICPMS. Four graduate students participated in this investigation. Three students have already graduated (one PhD in Nuclear Engineering, one MS in Nuclear Engineering, and one MS in Mechanical Engineering who is a minority student), while the fourth student continues to pursue his PhD degree in Nuclear Engineering.

6. REFERENCES

1. "Proceedings of the Axial Offset Anomaly (AOA) Workshop", EPRI Report TR-1000137, June 2000.
2. "PWR Axial Offset Anomaly (AOA) Guidelines, Revision 1," EPRI report TR-1000137, 2004.
3. "Boron-induced Offset Anomaly (BOA) Risk Assessment Tool," Version 1.0, User's Manual, EPRI Report #1003211 (April 2003).
4. "Experimental Verification of the Root Cause Mechanism for Axial Offset Anomaly," EPRI Report 1003212 (December 2002).
5. Bryappa, K., V. Rajeev, V. J. Hanumesh, A. R. Kulkarni, and A. B. Kulkarni, "Crystal Growth and Electrical Properties of Li2B4O7," Journal of Materials Research, 11(10), 2616-2621 (October 1996).
6. Kosinski, J. A., "New Piezoelectric Substrates for SAW Devices," International Journal of High Speed Electronics and Systems, 10(4), 1017-1068 (2000).

7. Wu, Zhibin, Masayuki Okuya, and Shoji Kaneko, "Spray Pyrolysis Deposition of Zinc Ferrite Films from Metal Nitrates Solutions" Thin Solid Films 385: 109-114 (2001).

8. Gautier, J.L., E. Rios, M. Gracia, J.F. Marco, and J.R. Gancedo, "Characterization by X-Ray Photoelectron Spectroscopy of Thin $Mn_xCo_{3-x}O_4$ ($1 \geq x \geq 0$) Spinel Films Prepared by Low-temperature Spray Pyrolysis" Thin Solid Films 311:51-57 (1997).

APPENDIX A

SPRAY PYROLYSIS APPARATUS

Spray pyrolysis was used to "pre-condition" the test elements during the early phases of this investigation. In this method a solution containing the desired ions is atomized and sprayed onto a heated substrate. The major components required for spray pyrolysis include:

- A low velocity atomizing nozzle
- A source of ion-bearing solution to supply the nozzle
- A flowmeter with a metering valve
- A substrate onto which the spray is deposited
- A method of heating the substrate (hot plate or AC variac)
- A thermocouple to monitor substrate temperature

A schematic of a typical spray pyrolysis set-up for a test wire is shown in Figure A-1.

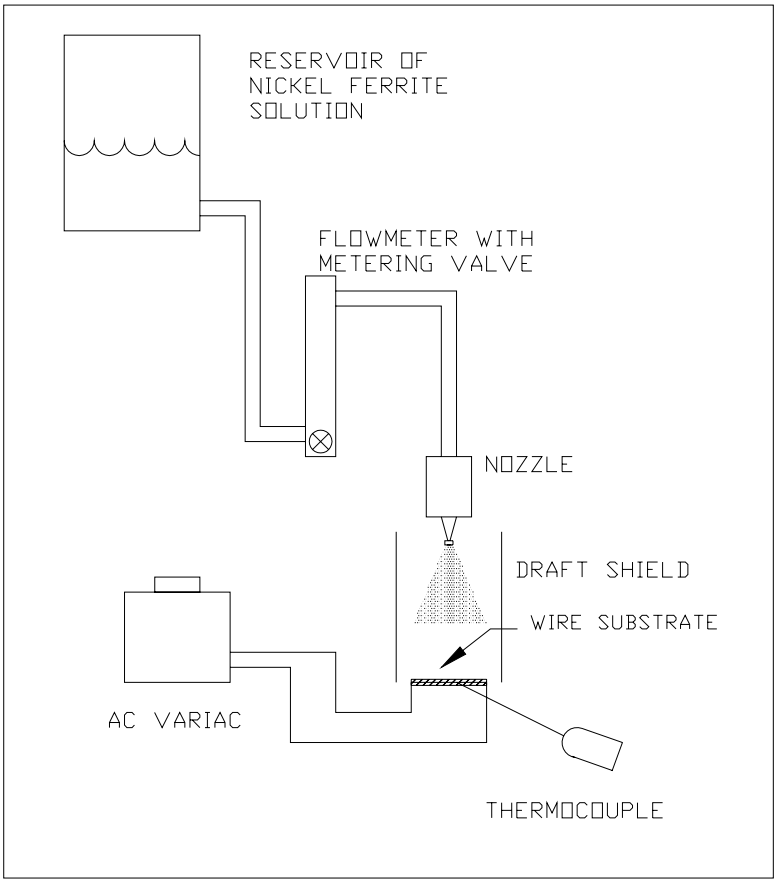

Figure A.1: Spray Pyrolysis Set-up

Two types of atomizing nozzles were tested: a cross-flow nebulizer nozzle and an ultrasonic nozzle. The nebulizer was prone to clogging and the compressed air stream used to atomize the liquid tended to cool down the substrate too much. The ultrasonic nozzle has several advantages over the nebulizer, all of which support the decision to abandon the nebulizer as the primary spraying device. The ultrasonic nozzle does not clog, does not require a forced airflow to produce droplets, and the nozzle dispenses more solution per unit time. Without the need of a pressurized air supply, the substrates experienced less heat loss. The nozzle operates by producing a soft, un-pressurized spray of small drops (mean drop size of approximately 40 μm). Since the ultrasonic atomization process does not rely on pressure, the amount of liquid atomized by a nozzle per unit time is primarily controlled by the liquid delivery system used in conjunction with a nozzle. Essentially, the droplets are produced by vibration energy absorbed by the solution, causing a liquid film forming on the nozzle tip to shatter into tiny droplets.

The first substrates used were glass microscope slides. They were chosen for their chemical inertness, ease of handling, and ease with which they could be examined using SEM, EDX, and XRD techniques. The glass slides were heated during the deposition process by placing them on a hot plate.

Pre-formed zircaloy-4 wires which could be placed in the pressure vessel were also used as substrates. These wires were resistively heated by connecting them to electrodes and applying a large current. Substrate temperature was monitored by placing a thermocouple in direct contact with the surface of the heated substrate.

A.1. SPRAY PYROLYSIS EXPERIMENTS

Prior to utilizing the configurations described above and running the experiments, the solution concentrations were calculated. From the literature and knowing that nickel ferrite has a 1:2 nickel to iron ratio, the concentration range of 0.02 M Ni^{2+} and 0.04 M Fe^{3+} was chosen. As summarized in Table A-1, it was determined that the solution would consist of 582 mg and 1620 mg of nickel and iron nitrates, respectively, dissolved in one liter of distilled water. The metal nitrate amounts were calculated for 100 mL of solution from the respective molecular weights and the chosen concentration. Final solutions were prepared by mixing $Ni(NO_3)_2 \cdot 6H_2O$ and $Fe(NO_3)_3 \cdot 9H_2O$ in 1:2 molecular weight proportions with 100 grams of distilled water.

The pH of the solution was measured using a Mettler Toledo DL50 Graphix automatic titration unit and found to be 1.99. This was done based on the recommendation of Wu, et al. [7], who concluded that solution pH strongly influenced the surface morphology of a coating/film when using spray pyrolysis deposition. The lattice parameter was found to increase when decreasing the solution pH and the crystallite size was directly proportional to the solution pH [7]. This information may be valuable in future tests in which the metal nitrate solution has varied pH levels.

Table A-1 – Solution Concentration Data

Metal Nitrate	Molecular Weight	1:2 Molar Ratio	Grams for 1 L	Grams for 100 mL
Nickel Nitrate	290.81 g/mol	0.02 M Ni^{2+}	5.8162 g	0.58162g
Ferric Nitrate	404.02 g/mol	0.04 M Fe^{3+}	16.1608 g	1.61608g

A.1.1. Nebulizer Experimental Procedure

The glass slides are cleaned with acetone and then weighed on a Sartorius balance to a hundred thousandths of a gram. After the slides are weighed, they are placed on the hot plate as it is warming; caution should be taken to prevent subjecting the slide to a large temperature gradient. An aluminum plate is placed between the slides and the hot plate to protect the heat source from the spray and to ease removal of the slides from the heat source once spraying is done. After the slide is coated by SPD for approximately 45-60 minutes, the weight is taken again to determine the amount of material deposited. The majority of material deposited should be nickel and iron as the water is expected to have evaporated before hitting the slide.

A.1.2. Ultrasonic Nozzle Experimental Procedure

A similar process as described in section A.1.1 is used for the slides during ultrasonic nozzle experiments. For preparation of the zircaloy test element, the wire is cut to the proper length and bent into the desired shape of test elements used in the pressure vessel experiments. After being bent, the wire ends are flattened to lower the contact resistance when the wire is installed in the spray pyrolysis apparatus as well as the pressure vessel. After the wire is shaped, it is cleaned in an Astrason Ultrasonic Cleaner bath with acetone (10 min. clean, 10 min. dry), weighed, and installed in the experimental setup.

The wire is then sprayed for about five hours, as a thick film is desired. The voltage and the substrate temperature are checked often for fluctuations. The wire temperature ranged from 400 to 500 ^{o}C. The solution level is checked often and additional solution is added to the reservoir as needed. After the wire is sprayed, cooled, and weighed, it is ready to be placed in the pressure vessel.

A.2. SPRAY PYROLYSIS EXPERIMENTS RESULTS

The results of applying the spray pyrolysis deposition (SPD) technique are described in this section. The section includes descriptions of results achieved with the nebulizer and the ultrasonic nozzle. Table A-2 summarizes the various experiments that were performed using the nebulizer (for slides only) and the ultrasonic nozzle (slides and wires). The table is comprised of the date a particular test was run, the substrate (glass or wire) used, device for spraying (nebulizer or ultrasonic nozzle), temperature of the substrate while sprayed, intermittent operation time in seconds, total duration of test in minutes, and results of the test (mainly denoting weight gain or substrate condition after test). Wires installed in the pressure vessel are not included in this table.

Figures A.2 through A.5 show microscope images of films deposited using spray pyrolysis. From these figures, one can notice the uniformity of the slide coatings, as the spray pyrolysis method is refined after each experiment. A difference is clearly visible between the slides sprayed with the nebulizer (Figures A.2 and A.3) and the slides sprayed with the ultrasonic nozzle (Figures A.4 and A.5). The slides sprayed with the nebulizer were sprayed with less material at lower temperatures. The annealed slide in Figure A.3 is dramatically different than

the slide in Figure A.2, both of which were sprayed the same day. Figure A.3 demonstrates the usefulness of annealing a substrate in order to support the formation of nickel ferrite. The variation is not only attributed to the nozzle but also the heat source, as the latter two slides were exposed to much higher temperatures (up to 300°C more) and display more of a crystalline structure. A ceramic hot plate replaced the previous aluminum hot plate for better performance. The slide in Figure A.5 was annealed for 5 hrs at approximately 400°C, after being sprayed with the solution of ferric and nickel nitrates.

The process is used as a means to advance the formation of a nickel ferrite coating. For reference, Gautier, et al. [8] annealed substrate films at 150°C for 60 minutes, in which a low temperature (150°C) spray pyrolysis was applied. An indication of crystallization occurring is a sign of nickel ferrite formation, seen in figures A.4 and A.5. Further analysis was done to be sure of the composition of the coating. With XRD, it was determined that $NiFe_2O_4$ formed on the annealed glass slide shown in Figure A.5. XRD analysis shows strong evidence that nickel ferrite is present, but there is also possible contamination of the spinel by nickel oxide.

Table A-2 – Summary of Spray Pyrolysis Experiments

Date	Substrate	Neb.	Ultra	Temp.(°C)	On/Off	Duration	Results
011403	Slide	X		160	--	30min	Gained 3.65mg
011603	Slide	X		190	30/30	80min	Gained 1.12mg
012303	Slide A	X		170	10,30/30	60min	Gained 3.92mg
012303	Slide B	X		80	--	40min	Gained 7.04mg*
012803	Slide	X		290	--	--	Shattered
020403	Slide		X	480	--	25min	Shattered
020603	Slide1		X	450-480	--	45min	Gained 2.09mg
020603	Slide2		X	450-480	--	45min	Shattered
021103	Slide1		X	245	--	60min	Gained 8.5mg
021103	Slide2		X	245	--	60min	Shattered
021103	Slide3		X	245	--	60min	Gained 6.35mg
021103	Slide4		X	245	--	60min	Shattered
021803	Slide**		X	350	--	90min	Gained 38.44mg*
022703	Wire1		X	250-300	--	170min	Gained 7.3mg, cont.
030603	Wire1		X	400-500	--	180min	Gained 90.42mg, 97.72
030703	Wire2		X	400-475	--	60min	Gained 19.7mg, cont.
031103	Wire2		X	450	--	210min	Cont., heater problem
031203	Wire2		X	480	--	120min	continued
031303	Wire2		X	450	--	195min	Gained 95.7mg
032503	Wire4		X	450	--	60min	Gained 58.98mg
032703	Wire5		X	400-500	--	60min	Gained 7.14mg

* Annealed later @ 400-450°C **Larger sized slide

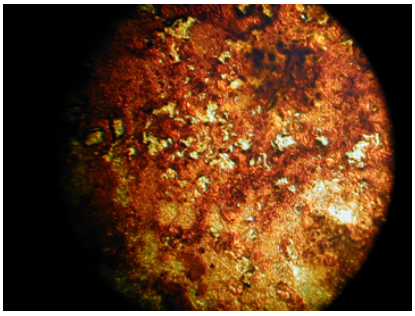

Figure A.2: Microscope Image of Coated Glass Slide (012303 A)

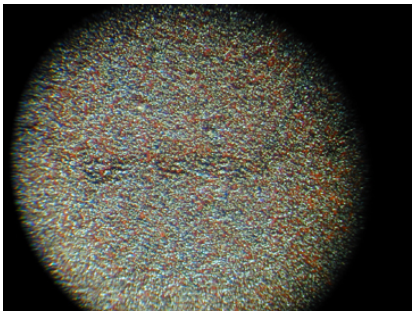

Figure A.4: Microscope Image of Coated Glass Slide (021103 1)

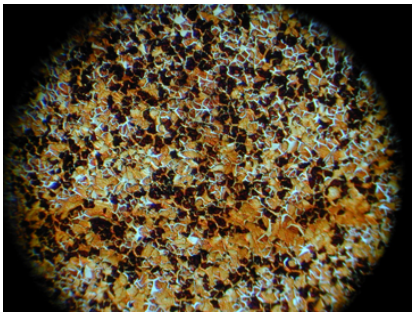

Figure A.3: Microscope Image of Annealed Slide (012303 B)

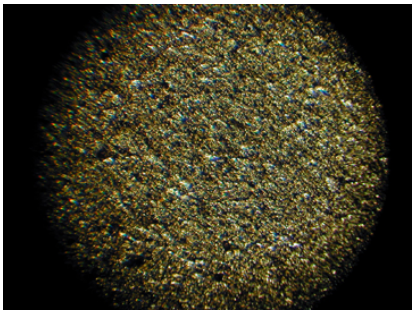

Figure A.5: Microscope Image of Annealed Slide (021803)

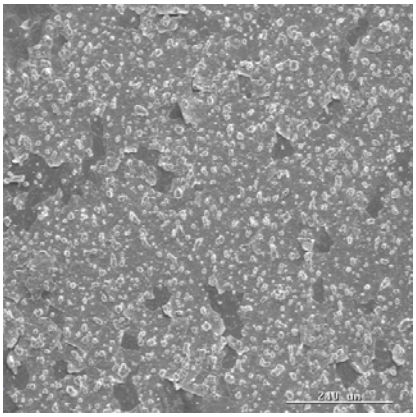

Figure A.6: SEM Image, Slide 021803 in Fe/Ni, Un-annealed

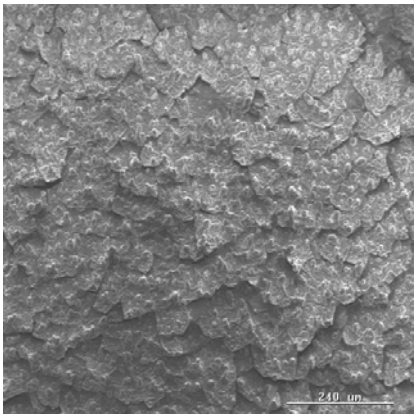

Figure A.7: SEM Image, Slide 021803

EDX analysis was performed for the slides shown in Figures A.6 and A.7. The images in these figures are actually fragments of one large slide that shattered into two parts as it was coated by SPD with the ultrasonic nozzle. The annealed slide displays a larger concentration of iron and nickel and very little evidence of silicone and calcium present in the un-annealed slide. Unlike XRD, the EDX data does not identify phases, but rather the elements within the coating composition. A 1:2 cation ratio of nickel to iron was found, which is very encouraging and supports the choice of the concentration. However, if this coating were pure nickel ferrite ($NiFe_2O_4$), one would expect to find a little more oxygen. Most likely the coating is a combination of nickel ferrite and oxides of nickel and iron.

The same analysis was carried out on the wire substrates. In Figure A.8, the SEM image of a heated, but unsprayed, wire is shown. As would be expected, the EDX data only shows zirconium and oxygen as opposed to the iron, nickel, oxygen, zirconium, and aluminum that are present within the sprayed wire coating. Figure A.9 is a photograph of a wire after being sprayed and Figure A.10 is an SEM image of the same wire. Figures A.8 and A.10 reveal large cracks both on the surface and in the coating covering the wires. These cracks indicate the coating may be brittle which contradicts the objective of producing a robust shell, needed if the wire is to be placed in the simulated PWR test vessel.

Two coated wires were tested in the pressure vessel with mixed results (see Table A.3). Wire 2 broke approximately seven days after being weighed and installed in the pressure vessel. Wire 4 (Figure A.11) shattered after 105 minutes within the vessel. For comparison, wires that are not sprayed are generally kept in the vessel for weeks or even months without breaking. Considering the amount of stress the wires are subjected to during SPD indicates the wires are not robust enough to survive the harsh environment of the test vessel. The pressure vessel simulates PWR primary coolant pressures and temperatures, which are approximately 2000 psig and 590°F, respectively. The electrically-heated wires are maintained at surface heat fluxes up to 5×10^5 Btu/hr-ft^2 (~1.6 MW/m^2).

The most promising result from the pressure vessel tests is the increased rate of accumulation of material on the wire. A wire treated with the spray pyrolysis technique exhibited a significant amount of deposited material as opposed to a wire without the treatment, within a shorter time period as well. The accumulation of material may be attributed to the "seed" theory – the presence of a small amount of the desired material seems to attract more of the same.

XRD analysis of Wire 2, an example of a wire installed in the vessel that exhibited the "seed" theory, was performed. The results reveal the presence of cuprite (Cu_2O), lithium iron nickel oxide ($Li_2NiFe_2O_4$), copper borate (CuB_2O_4), tenorite (CuO), and most importantly, nickel ferrite ($NiFe_2O_4$). The source of the copper may be attributed to corrosion, within the test vessel, of the electrodes used for heating the wire substrates.

Based on the results obtained with SPD, it was concluded that in-situ crud formation by adding soluble and insoluble nickel and iron compounds in the vessel (see Section 3 of the report) was preferable, inasmuch as one can reliably produce crud with prototypical composition, and morphology at extremely high rates which allow meaningful experiments to be conducted at reasonable durations (few days to few weeks).

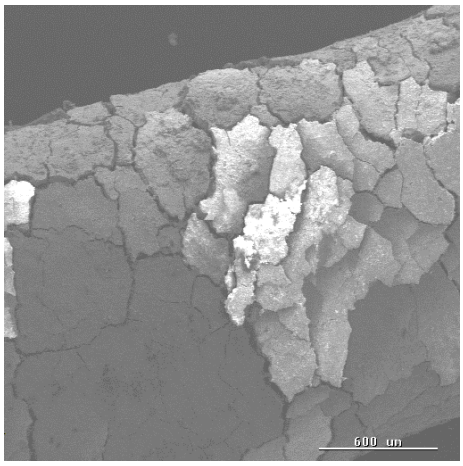

Figure A.8: Wire 3 (030603) Heated 450°C without Solution

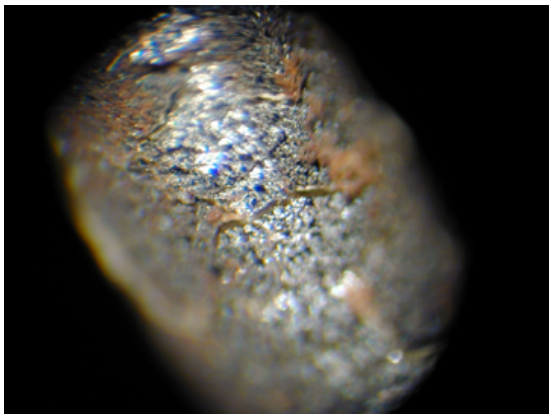

Figure A.9: Magnified Image of Zircaloy Wire 1

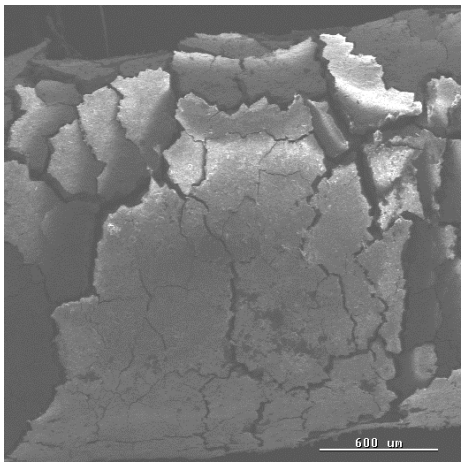

Figure A.10: Wire 1 (030603 Heated 450°C with Solution

Zircaloy Wires					
Weights	W1	W2	W3*	W4	W5
Uncoated	2.20528g	2.57350g	2.18545g	2.37294g	2.41840g
Coated	2.30300g	2.66920g	2.19495g	2.43189g	2.42554g
Coating Gain	0.09772g	0.09570g	0.00950g	0.05895g	0.00714g
Post Vessel	--	2.79387g	--	2.42900g**	--
Crud Gain	--	0.12467g	--	-0.00289g	--
Total Gain	**0.09772g**	**0.22037g**	**0.00950g**	**0.05606g**	**0.00714g**

*heated only, not coated
**small portion of coating deteriorated in vessel

Figure A.11: Wire 4 after Shattering in Vessel